Published in final edited form as:
Exp Hematol. 2014 December ; 42(12): 1059–1067. doi:10.1016/j.exphem.2014.09.002.

mRNA Regulation of Cardiac Iron Transporters and Ferritin Subunits in a Mouse Model of Iron Overload

Casey J. Brewer, BS[1], **Ruth I. Wood, PhD**[2], and **John C. Wood, MD, PhD**[1]

[1]Division of Pediatric Cardiology, Children's Hospital Los Angeles, CA

[2]Department of Cell and Neurobiology, Keck School of Medicine of the University of Southern California, Los Angeles, CA

Abstract

Iron cardiomyopathy is the leading cause of death in iron overload. Men have twice the mortality rate of women, though the cause is unknown. In hemojuvelin-knockout mice, a model of the disease, males load more cardiac iron than females. We postulated that sex differences in cardiac iron import cause differences in cardiac iron concentration. RT-PCR was used to measure mRNA of cardiac iron transporters in hemojuvelin-knockout mice. No sex differences were discovered among putative importers of non-transferrin bound iron (L-type and T-type calcium channels, ZRT/IRT-like protein 14 zinc channels). Transferrin-bound iron transporters were also analyzed; these are controlled by the iron regulatory element/iron regulatory protein (IRE/IRP) system. There was a positive relationship between cardiac iron and ferroportin mRNA in both sexes, but it was significantly steeper in females ($p<0.05$). Transferrin receptor 1 and divalent metal transporter 1 were more highly expressed in females than males ($p<0.01$ and $p<0.0001$, respectively), consistent with their lower cardiac iron levels, as predicted by IRE/IRP regulatory pathways. Light-chain (L) ferritin showed a positive correlation with cardiac iron that was nearly identical in males and females ($R^2=0.41$, $p<0.01$ and $R^2=0.56$, $p<0.05$, respectively), while heavy-chain (H) ferritin was constitutively expressed in both sexes. This represents the first report of IRE/IRP regulatory pathways in the heart. Transcriptional regulation of ferroportin was suggested in both sexes, creating a potential mechanism for differential set points for iron export. Constitutive H-ferritin expression suggests a logical limit to cardiac iron buffering capacity at levels known to produce heart failure in humans.

Keywords

iron overload; heart; ferroportin; ferritin; iron-regulatory proteins

Address for Correspondence Dr. John Wood, MD, PhD, Division of Cardiology, Mailstop 34, Children's Hospital Los Angeles, 4650 Sunset Blvd, Los Angeles, CA, 90027-0034, 323 361 5470 (Phone), 323 361 7317 (FAX), jwood@chla.usc.edu.

FINANCIAL DISCLOSURE DECLARATION
The authors have no other financial or personal relationship with organizations that could potentially be perceived as influencing the described research.

INTRODUCTION

While iron is essential for many of the body's processes, excess iron produces oxidative stress, leading to vascular and organ damage. Iron overload can be caused by genetic mutations to iron regulatory genes (primary iron overload, i.e. hemochromatosis) or by chronic blood transfusions during the treatment of hemoglobinopathies such as thalassemia (secondary iron overload) [1-3]. Despite current treatments, iron-mediated cardiomyopathy remains the leading cause of death in thalassemia [4]. Female thalassemia patients have a two-fold greater survival rate than males [5]; similar disparities in disease severity have been documented in hereditary hemochromatosis [6]. The reason for this is unknown.

Previously, we explored this sex difference in a hemojuvelin knockout mouse; this juvenile hemochromatosis model produces cardiac iron levels and distribution similar to humans [7]. Animals of both sexes were gonadectomized and received Silastic implants filled with testosterone, dihydrotestosterone, estrogen, or cholesterol (as a control). Regardless of treatment, males exhibited significantly greater heart iron concentrations than females. In addition, sex steroid treatment significantly increased cardiac iron concentration in males, but not in females. In particular, gonadectomized males with estrogen replacement had significantly more heart iron than gonadectomized males with a control cholesterol implant; estrogen did not cause a similar increase in female heart iron [8]. We concluded that postnatal steroids, acting through an activational estrogenic mechanism, were responsible for increasing cardiac iron. However, prenatal steroid exposure, prior to gonadectomy, must also be producing organizational changes in iron metabolism because the activational effects were only seen in males.

The present study pursues potential mechanisms for the sex differences seen in cardiac iron loading in this model. We analyzed the mRNA of three suspected nontransferrin bound iron (NTBI) transporters: L-type calcium channels, T-type calcium channels, and ZRT/IRT-like protein 14 (*Zip14*) zinc channels [9-11]. We also probed for evidence of iron regulatory circuits in the heart. Classically, transferrin-bound iron importers and exporters are regulated via the iron regulatory element/iron regulatory protein (IRE/IRP) system [12]. These transporters contain IREs in their mRNA that are bound by IRPs –translation of the mRNA can then be regulated in response to changes in cellular iron. It is possible that sex differences in the regulation of these transporters could influence cardiac iron levels; we therefore analyzed the mRNA of the iron exporter ferroportin, the iron importers transferrin receptor 1 (*Tfr1*) and divalent metal transporter 1 (*Dmt1*), and the iron storage protein ferritin. Organ iron homeostasis has been previously examined, most often in the duodenum, liver and macrophages, but this represents the first description of cardiac iron homeostasis in a mouse model of iron overload.

METHODS

Animals

Mice were housed in the Animal Care Facility of Children's Hospital Los Angeles. All studies were carried out with approval of the Institutional Animal Care and Use Committee

of Children's Hospital Los Angeles. Hemojuvelin knockout mice (*Hjv*−/−) were used to induce dietary iron overload; these mice have the background strain of 129S6/SvEvTac and were obtained from the lab of Dr. Nancy Andrews at Children's Hospital Boston [13]. To probe for hormonal effects, mice were gonadectomized and received hormone implants. Female mice were ovariectomized (OVX) and male mice were castrated (OrchX) at 4 weeks of age. Female mice received either an estrogen implant (OVX + E) or a cholesterol control (OVX); males received an implant containing testosterone (OrchX + T), DHT (OrchX + DHT), estrogen (OrchX + E), or cholesterol (OrchX). Intact males and females received a sham gonadectomy and a cholesterol control implant. There were 7 mice per group; the OVX and OrchX groups had 12 mice per group. The mice were placed on a high iron diet for the 8 weeks following gonadectomy (1400 ppm iron; Newco Distributors, Rancho Cucamonga, CA, USA). A high-iron diet was necessary to overcome the rodents' upregulation of iron excretion during iron overload, a phenomena that is not seen in humans. Also, a high-iron diet allowed for the development of cardiac iron loading in a short period of time. At 12 weeks of age, the mice were sacrificed and the heart and liver tissue were harvested. Except for ferroportin, significant effects of hormone treatment were not observed on any of the genes that were analyzed. Therefore, data from the hormone treatment groups were pooled by sex and compared to heart iron concentration.

Gonadectomy and hormone implants

All surgeries were performed under Avertin anesthesia (250 mg/kg). Orchiectomy was performed via midline scrotal incision and ovariectomy was performed through bilateral dorsal flank incisions. Steroids were replaced at physiological levels by Silastic implant subcutaneously. Males and females received a 5-mm implant (outer diameter, 2.16 mm; inner diameter, 1.02 mm; Dow Corning, Midland, MI, USA) filled with crystalline steroid (Steraloids, Newport, RI, USA). Estradiol was first mixed with cholesterol before being loaded into the implant (1:1 17β-estradiol:cholesterol). These implants have been shown to restore normal male and female phenotypes in numerous previous studies [14-17].

Iron quantification

Heart and liver specimens were digested in 100% nitric acid at 80°C for 10 minutes; an equal volume of 30% H_2O_2 was then added, and digestion continued at 80°C for an additional 10 minutes or until the tissue was dissolved completely. Digested samples were diluted with reagent-grade water to 2% nitric acid concentration and analyzed by flame atomic absorption spectrophotometry (Perkin Elmer, Waltham, MA, USA).

Reverse transcription-polymerase chain reaction

RNA was extracted using the RNeasy Protect Mini Kit (Qiagen, Valencia, CA, USA). Tissues were excised and submerged in RNA Later solution immediately after sacrifice. Tissue samples in RNA Later solution were stored at −20°C until RNA extraction was performed. Complementary DNA was synthesized using the SuperScript III First-Strand Synthesis System (Invitrogen, Carlsbad, CA, USA). Reverse transcription-polymerase chain reactions (RTPCRs) were done using the Power SYBR Green PCR Master Mix (Applied Biosystems, Carlsbad, CA, USA). Samples were run on a 7900 HT Fast Real-Time PCR

System (Applied Biosystems, Carlsbad, CA, USA). Linearity of amplification was verified for all primers. Gene expression was reported relative to glyceraldehyde-3-phosphate dehydrogenase (Gapdh) expression. Relative expression values were derived from Delta Ct using the following formula: Gene expression relative to Gapdh = 2^(-Delta Ct). *Hamp1* expression was reported relative to β-actin via the same formula. Primer sequences were as follows: *Zip14* forward, 5-GAGCCAACTGATAATCCATTGCT-3; *Zip14* reverse, 5-GTCAACGGCCACATTTTCAA-3 [18]; L-type calcium channel forward, 5-GATGGGATCATGGCTTATGG -3; L-type calcium channel reverse, 5-GGCCAGCTTCTTTCTCTCCT-3 [19]; T-type calcium channel forward, 5-ACCCTCCCCAAAGAAAGAT-3; T-type calcium channel reverse, 5-GCTTACATGGGACTTTTCAG-3 [20]; Gapdh forward, 5-CAATGTGTCCGTCG TGGATCT-3; Gapdh reverse, 5-GTCCTCAGTGTAGCCCAAGATG-3 [21]; ferroportin forward, 5-TGGATGGGTCCTTACTGTCTGCTAC-3; ferroportin reverse, 5-TGCTAATCTGCTCCTGTTTTCTCC-3 [22]; *Tfr1* forward, 5-TCCCGAGGGTTATGTGGC-3; *Tfr1* reverse, 5-GGCGGAAACTGAGTATGATTGA-3 [23]; *Dmt1* forward, 5-TCAGAGCTCCACCATGACTG-3; *Dmt1* reverse, 5-TGTGAACGTGAGGATGGGTA-3 [24]; L-ferritin forward, 5-TGGCCATGGAGAAGAACCTGAATC-3; L-ferritin reverse, 5-GGCTTTCCAGGAAGTCACAGAGAT-3 [25]; H-ferritin forward, 5-GATCAACCTGGAGTTGTATGCC-3, H-ferritin reverse, 5-CTCCCAGTCATCACGGTCTG-3 [26]; *Dmt1* IRE-negative forward, 5-CGCCCAGATTTTACACAGTG-3; *Dmt1* IRE-negative reverse, 5-TTGGAGTGTCGGTGCTTAAA-3 [27]; *Dmt1* IRE-positive forward, 5-TGTTTGATTGCATTGGGTCTG-3; *Dmt1* IRE-positive reverse, 5-CGCTCAGCAGGACTTTCGAG-3 [28]; *Hamp1* forward, 5-CTGAGCAGCACCACCTATCTC-3, *Hamp1* reverse 5-TGGCTCTAGGCTATGTTTTGC-3 [29]; β-actin forward 5-GACGGCCAGGTCATCACTATTG-3, β-actin reverse 5-CCACAGGATTCCATACCCAAGA-3 [29].

Statistical analysis

All statistical tests were performed using JMP 5.1 (SAS Institute, Cary, NC, USA). Because hormone treatment groups differed in males and females, hormone effects were evaluated in each sex separately by 1-way analysis of variance (ANOVA). When no treatment group differences were observed, data were pooled across sex and analyzed by Student's t test; data were log-transformed when appropriate. Significance of linear correlations was defined as a p value < 0.05. Discriminant analysis was used to demonstrate the separation of male and female data in the ferroportin vs. heart iron comparison.

RESULTS

Table 1 summarizes iron levels, organ and body weights, and *Hamp1* expression in the study animals (*Hjv*−/−). Reference ranges for wild type control animals are shown for comparison (strain 129S6/SvEvTac). Hepatic iron concentrations were increased 5-9 fold from wild type animals. Cardiac iron increased threefold in males and twofold in females compared to wild

type. *Hamp1* levels were on average 1.5x higher in *Hjv* −/− females than in *Hjv* −/− males, but this difference was not significant (p=0.19). High residual *Hamp1* expression was limited to intact *Hjv*−/− females (Figure 1); *Hamp1* expression in the OVX and OVX+E females was the same as for males. *Hjv* −/− males and females had less than 10% the *Hamp1* expression of their wild type counterparts (Table 1). There was no correlation between *Hamp1* and heart iron concentration (data not shown). In estrogen-treated animals, *Hamp1* expression was lower in females than in males (0.7 ± 1.6 versus 1.7 ± 2.0 relative to Gapdh, $p<0.05$), yet estrogen-treated females had significantly lower cardiac iron than estrogen treated-males (172 ± 21 versus 290 ± 69 ug/g wet weight, $p<0.01$). Thus, sex differences in cardiac iron cannot be attributed to differences in *Hamp1* expression.

No effect of sex (Table 2, “expression relative to Gapdh”) or hormone treatment (Table 2, “hormone effect”) was observed for mRNA of L-type calcium channels, T-type calcium channels, or *Zip14* zinc channels. Furthermore, no association was seen between cardiac iron levels and the channels’ mRNA levels (Table 2, “correlation with heart iron concentration”). These data support the hypothesis that cardiac iron uptake of NTBI is constitutive once transferrin becomes completely saturated.

However, steady-state cardiac iron concentration reflects a balance between intake and export. Thus we analyzed the iron exporter ferroportin for possible sex differences. This channel is the sole known mammalian exporter of tissue iron and has been shown to regulate intracellular iron levels through the IRE/IRP system [12, 30]. In males, there was a correlation between heart iron concentration and ferroportin mRNA expression ($R^2=0.35$, $p<0.01$). Females showed a similar trend, though the correlation did not reach statistical significance because of a single outlier ($R^2=0.12$, $p<0.22$ with outlier, $R^2=0.50$, $p<0.01$ without outlier; outlier indicated by arrow, Figure 2). Interestingly, ferroportin increased more sharply in females in response to cardiac iron overload, potentially limiting cardiac iron accumulation. The separation of the male and female ferroportin response was significant by discriminate analysis ($p<0.05$). The observed sex difference could represent a difference in set point (x-intercept), a difference in strength of response (slope), or both; this study was underpowered to distinguish among these possibilities. Ferroportin did show significantly higher expression in OrchX+E mice compared to OrchX (0.0026 versus 0.00087 relative to Gapdh, $p<0.05$), but OrchX+E mice also had significantly more heart iron than OrchX mice (289.6 versus 195.6 ug/g, $p<0.05$). In females, estrogen treatment had no effect on heart iron concentration or ferroportin mRNA expression. Therefore, estrogen's effect on ferroportin expression in males was likely secondary to estrogen's effect on heart iron concentration.

Since we saw sex differences in IRE/IRP regulated iron exporter mRNA, it was logical to probe the IRE/IRP controlled importers, *Tfr1* and *Dmt1*, for sex differences as well. The classic model of IRE/IRP regulation predicts that these importers’ mRNA will be degraded when iron levels are high [12, 31]. In our study, cardiac *Tfr1* levels were lower in males than in females relative to Gapdh ($3.3*10^{-4}$ vs. $6.8*10^{-4}$, respectively, $p<0.01$) (Figure 3A). *Tfr1* was also negatively correlated with heart iron concentration ($R^2=0.16$, $p<0.05$) (Figure 3B). No significant hormone effects were observed. Cardiac *Dmt1* levels were also lower in males than in females relative to Gapdh ($1.1*10^{-3}$ vs. $1.8*10^{-3}$, respectively, $p<0.0001$)

(Figure 4A). Interestingly, males showed a positive correlation between heart iron concentration and *Dmt1* mRNA (R^2=0.25, p<0.05) (Figure 4B). Despite this paradoxical positive correlation, the total level of *Dmt1* mRNA in males was quite low. Taken together, these results are consistent with classical IRE/IRP regulation, with decreased *Tfr1* and *Dmt1* mRNA levels when cellular iron levels are high, thereby limiting cellular iron intake.

Dmt1 is known to have multiple splice variants, some with a 3' IRE ("IRE-positive") and some without ("IRE-negative"). mRNA for both isoforms was detected in the cardiac tissue of our mice, with IRE-positive *Dmt1* more highly expressed than the IRE-negative isoform. Females had significantly more IRE-positive *Dmt1* mRNA than males (0.00060 vs. 0.00049 respectively, relative to Gapdh, p<0.05). IRE-negative *Dmt1* mRNA was expressed at a low level in females and males (0.00015 vs. 0.00013 respectively, relative to Gapdh, p=0.50) (Figure 5).

To complete the characterization of the cardiac IRE/IRP circuit, we analyzed mRNA expression of the iron storage genes, light-chain (L) and heavy-chain (H) ferritin, relative to Gapdh. Males and females showed very similar positive correlations of L-ferritin mRNA with heart iron concentration (R^2=0.41, p<0.01 for males and R^2=0.56, p<0.05 for females) (Figure 6). H-ferritin mRNA levels were about 2-7 fold higher than those of L-ferritin in both males and females. There was no correlation seen between heart iron concentration and H-ferritin mRNA; instead, H-ferritin was constitutively expressed (Figure 7A). Interestingly, when normalized to heart iron concentration, females expressed significantly more H-ferritin mRNA than males (0.0022 vs. 0.0013, respectively, p<0.001) (Figure 7B).

DISCUSSION

Most previous research into cardiac iron overload has focused on putative NTBI import channels. While these importers are important because they represent a potential therapeutic target, we did not observe any sex differences in their message level. In contrast, we noted differential regulation of the iron exporter ferroportin consistent with observed sex differences in cardiac iron. While we could not distinguish whether females had a lower cardiac iron setpoint for ferroportin upregulation, a steeper slope between ferroportin message and cardiac iron, or both, our data suggests that regulation of iron export could be an underappreciated determinant of cardiac iron accumulation.

We did not have sufficient tissue for Western blot analysis or ferroportin localization studies to confirm or refute functional significance of our observed mRNA changes. However, strong ferroportin induction by cardiac iron could explain several phenomena observed in mice and in humans. First, cardiac iron overload appears to be self-limiting in many murine models, such that cardiac iron levels plateau over time [13]. In humans, there is a long latency between hepatic iron loading and cardiac iron loading. The mechanism for this latency period is poorly understood, but it is possible that cardiac iron export is able to balance NTBI influx over certain ranges. However, once cardiac iron loading begins, it generally proceeds very rapidly [32] suggesting a saturation phenomenon to the compensatory mechanisms. Additional support for this hypothesis is the relatively low rate of cardiac iron loading in thalassemia intermedia. Circulating NTBI levels are increased in

thalassemia intermedia but the molar flux of these labile iron species is significantly lower than in transfusional siderosis. We postulate ferroportin iron export can successfully balance NTBI uptake over the flux rates observed in thalassemia intermedia for many years. However, once ferroportin expression is maximized, cardiac iron accumulation can be quite rapid.

In the classic models, IRE/IRP regulation of ferroportin is translational, not transcriptional, through binding to the 5' untranslated region [12]. Translational regulation has been demonstrated in such tissues as the liver and duodenum [12], but has not been explored in the heart. In the present study, we observed that ferroportin mRNA increases with cardiac iron, suggesting transcriptional as well as possible translational control of ferroportin upregulation in the heart. While the mechanisms of transcriptional control are not clear, other groups have shown that ferroportin transcription in macrophages can be regulated by heme [33, 34]; other studies in macrophages and lung cells have shown ferrportin transcription to be increased by high cellular iron concentration [35, 36]. These mechanisms are of clinical interest because potentiating cardiac ferroportin upregulation could be a useful therapeutic target.

Since females had lower cardiac iron than males, the IRE/IRP system was expected to promote stabilization of their *Dmt1* and *Tfr1* mRNA, as was observed. *Tfr1* also displayed a negative relationship with heart iron in both sexes. While these responses are intuitive based on classic IRE/IRP regulation, this is the first manuscript to describe these findings in the heart. The female *Tfr1* response may have had a steeper relationship with iron compared to males, similar to ferroportin, but we did not have sufficient range of cardiac iron levels in females to explore this hypothesis.

While male *Dmt1* mRNA was low compared to females, males did show a paradoxical positive correlation between *Dmt1* expression and heart iron concentration. *Dmt1* exhibits multiple transcripts, some containing an IRE ("IRE-positive") and some without ("IRE-negative") [37]. In theory, as cardiac iron levels increase, IRE-positive transcripts would be degraded but IRE-negative transcripts would be unaffected. Males with increased constitutive IRE-negative *Dmt1* expression would potentially take up more circulating NTBI, creating a positive correlation between heart iron and *Dmt1*. While the presence of IRE-positive and IRE-negative *Dmt1* mRNA was detected in the hearts of our mice, correlations were not seen between the mRNA expression and heart iron concentration. This may be due to the low expression level of the two isoforms, or because of differences at the protein level. Regardless, since males have considerably less total *Dmt1* mRNA than females, differences in IRE-negative *Dmt1* mRNA are likely to be of little importance with respect to influencing cardiac iron levels.

Further evidence of IRE/IRP mediated cardiac iron homeostasis was demonstrated by the regulation of L-ferritin by cardiac iron. Safe tissue packaging of cellular iron is accomplished by the ferritin protein, a sphere-like shell composed of 24 H and L ferritin subunits. The L:H ratio of the ferritin molecule varies according to tissue type; L-rich ferritin is abundant in iron-storage organs such as the liver and spleen while H-rich ferritin is found in organs of low iron content such as the heart and brain [38]. While L-rich protein

has prolonged turnover time and is more resistant to proteolysis than H-rich protein [39], it is the H-ferritin subunit that possesses the ferroxidase ability required for a functional ferritin molecule [40, 41]. In normoxic conditions, the translational control of L and H-ferritin subunits is similar, with translational repression occurring when iron concentration is low [42]. Transcriptional control of the two subunits is not as well studied, but work in the rat liver has shown L-ferritin transcription increases with iron while H-ferritin transcription does not rise significantly [43]. Examination of the L-ferritin promoter has shown it to be affected by antioxidant inducers as well as high iron concentrations; the H-ferritin promoter did not show the same response to high iron [44]. In a separate study, L-ferritin mRNA was found to be twice as high in old rat hearts compared to young ones, presumably upregulated by age-related oxidative stress, while H-ferritin levels did not change [45]. Taken together, these findings coincide with what we saw in the mouse heart, as L-ferritin mRNA correlated with heart iron concentration while H-ferritin mRNA was constitutively expressed.

However, the constitutive transcription of H-ferritin appears to be limiting at high iron concentrations. H-ferritin is the only known cytoplasmic ferroxidase capable of converting Fe^{2+} to Fe^{3+}, and tight regulation of H-ferritin is believed to be necessary for quick chelation of labile iron and prevention of oxidative stress [40]. Based on Figure 6, one would predict that the L:H ratio of cardiac ferritin protein would surpass 1 near cardiac iron levels of 800 μg/g wet weight, or roughly 4.8 mg/g dry weight [46, 47]. In humans, cardiac iron levels of this magnitude correspond to a cardiac T2* value of 6.3 milliseconds and are associated with a 50% risk of developing heart failure in one year [48]. While L-rich ferritin is favorable for long-term iron storage, it is not as well-suited for quick iron clearance. Our data therefore suggests that heart failure in iron overloaded patients occurs when cardiac iron accumulation outstrips the iron detoxification capacity provided by H-rich ferritin. For this reason, the regulatory mechanisms of cardiac H-ferritin are potentially attractive therapeutic targets.

Sex differences in cardiac iron loading have been previously described. J. Krijt et al. showed that hemojuvelin knockout females have 10-fold more *Hamp1* expression than hemojuvelin knockout males, which could potentially affect NTBI and therefore cardiac iron [49]. More recent work by C. Latour et al. showed that *Bmp6* knockout females also have more residual *Hamp1* expression than males, and that the females did not develop cardiac iron overload while the males did [50]. However, the female hemojuvelin knockout mice in our study had much lower residual *Hamp1* expression than found in either of the two prior studies, with increased expression (but still <10% of wild type) only in gonad intact females. Thus, while residual *Hamp1* expression may have accounted for previous observations made in other labs, it cannot explain sex differences in cardiac iron observed in our study.

C. Latour et al. also reported that hepcidin-deficient (*Hamp* −/−) males and females both developed cardiac iron overload, as in the present study. No sex difference was described and iron quantification was not performed, but Prussian blue staining shown in the supplemental data clearly suggests increased pancreatic and cardiac iron loading in the males (Figure S4)[50]. Thus, while near complete hepcidin suppression places a permissive role in cardiac iron loading, factors other than *Hamp1* expression are responsible for observed sex differences in extrahepatic iron loading.

The primary limitation of this study is the lack of protein work to independently assess translational and transcriptional regulation. Determination of cardiac iron levels by atomic absorption required substantial amounts of the ventricle and the rest of the ventricular tissue was needed for the RT-PCR work. We chose to focus on the RT-PCR data because we could analyze a wide range of iron transporters and rapidly screen for sex differences and interactions with cardiac iron burden. However, we recognize that further studies probing the mechanisms of cardiac ferroportin and ferritin subunit regulation through the IRE/IRP system will need protein validation of observed changes in mRNA levels.

Acknowledgments

SUPPORT

Partial funding for this study was provided by the National Heart, Lung, and Blood Institute (grant no. 1RC HL099412-01) and by Novartis. Dr. John C. Wood consults for Shire, ApoPharma, and Novartis, and has received speaker's honoraria and travel support from all three companies.

LITERATURE CITED

1. Bolondi G, Garuti C, Corradini E, et al. Altered hepatic BMP signaling pathway in human HFE hemochromatosis. Blood Cells Mol Dis. 2010; 45:308–312. [PubMed: 20863724]
2. Papanikolaou G, Samuels ME, Ludwig EH, et al. Mutations in HFE2 cause iron overload in chromosome 1q-linked juvenile hemochromatosis. Nat Genet. 2004; 36:77–82. [PubMed: 14647275]
3. Porter JB. Pathophysiology of Transfusional Iron Overload: Contrasting Patterns in Thalassemia Major and Sickle Cell Disease. Hemoglobin. 2009; 33:S37–S45. [PubMed: 20001631]
4. Wood JC, Kang BP, Thompson A, et al. The effect of deferasirox on cardiac iron in thalassemia major: impact of total body iron stores. Blood. 2010; 116:537–543. [PubMed: 20421452]
5. Borgna-Pignatti C, Rugolotto S, De Stefano P, et al. Survival and complications in patients with thalassemia major treated with transfusion and deferoxamine. Haematologica. 2004; 89:1187–1193. [PubMed: 15477202]
6. Burke W, Thomson E, Khoury M, et al. Hereditary hemochromatosis: Gene discovery and its implications for population-based screening. JAMA. 1998; 280:172–178. [PubMed: 9669792]
7. Otto-Duessel M, Brewer C, Wood JC. Interdependence of cardiac iron and calcium in a murine model of iron overload. Transl Res. 2011; 157:92–99. [PubMed: 21256461]
8. Brewer C, Otto-Duessel M, Wood RI, Wood JC. Sex differences and steroid modulation of cardiac iron in a mouse model of iron overload. Transl Res. 2014; 163:151–159. [PubMed: 24018182]
9. Oudit GY, Sun H, Trivieri MG, et al. L-type Ca(2+) channels provide a major pathway for iron entry into cardiomyocytes in iron-overload cardiomyopathy. Nat Med. 2003; 9:1187–1194. [PubMed: 12937413]
10. Kumfu S, Chattipakorn S, Srichairatanakool S, Settakorn J, Fucharoen S, Chattipakorn N. T-type calcium channel as a portal of iron uptake into cardiomyocytes of beta-thalassemic mice. Eur J Haematol. 2010; 86:156–166. [PubMed: 21059103]
11. Nam H, Wang C, Zhang L, et al. ZIP14 and DMT1 in the liver, pancreas, and heart are differentially regulated by iron deficiency and overload: implications for tissue iron uptake in iron-related disorders. Haematologica. 2013; 98:1049–1057. [PubMed: 23349308]
12. Muckenthaler MU, Galy B, Hentze MW. Systemic Iron Homeostasis and the Iron-Responsive Element/Iron-Regulatory Protein (IRE/IRP) Regulatory Network. Annu Rev Nutr. 2008; 28:197–213. [PubMed: 18489257]
13. Huang FW, Pinkus JL, Pinkus GS, Fleming MD, Andrews NC. A mouse model of juvenile hemochromatosis. J Clin Invest. 2005; 115:2187–2191. [PubMed: 16075059]

14. Wersinger SR, Sannen K, Villalba C, Lubahn DB, Rissman EF, De Vries GJ. Masculine sexual behavior is disrupted in male and female mice lacking a functional estrogen receptor alpha gene. Horm Behav. 1997; 32:176–183. [PubMed: 9454668]
15. Antzoulatos E, Jakowec MW, Petzinger GM, Wood RI. Sex differences in motor behavior in the MPTP mouse model of Parkinson's disease. Pharmacol Biochem Behav. 2010; 95:466–472. [PubMed: 20347863]
16. Jacob DA, Temple JL, Patisaul HB, Young LJ, Rissman EF. Coumestrol antagonizes neuroendocrine actions of estrogen via the estrogen receptor alpha. Exp Biol Med. 2001; 226:301–306.
17. Barkley MS, Goldman BD. The effects of castration and Silastic implants of testosterone on intermale aggression in the mouse. Horm Behav. 1977; 9:32–48. [PubMed: 561020]
18. Liuzzi JP, Bobo JA, Lichten LA, Samuelson DA, Cousins RJ. Responsive transporter genes within the murine intestinal-pancreatic axis form a basis of zinc homeostasis. Proc Natl Acad Sci U S A. 2004; 101:14355–14360. [PubMed: 15381762]
19. Golden KL, Marsh JD, Jiang Y. Castration reduces mRNA levels for calcium regulatory proteins in rat heart. Endocrine. 2002; 19:339–344. [PubMed: 12624436]
20. Mizuta E, Miake J, Yano S, et al. Subtype switching of T-type Ca 2+ channels from Cav3.2 to Cav3.1 during differentiation of embryonic stem cells to cardiac cell lineage. Circ J. 2005; 69:1284–1289. [PubMed: 16195632]
21. Vecchi C, Montosi G, Zhang K, et al. ER stress controls iron metabolism through induction of hepcidin. Science. 2009; 325:877–880. [PubMed: 19679815]
22. Van Zandt KE, Sow FB, Florence WC, et al. The iron export protein ferroportin 1 is differentially expressed in mouse macrophage populations and is present in the mycobacterial-containing phagosome. J Leukoc Biol. 2008; 84:689–700. [PubMed: 18586980]
23. Huang ML, Becker EM, Whitnall M, Suryo Rahmanto Y, Ponka P, Richardson DR. Elucidation of the mechanism of mitochondrial iron loading in Friedreich's ataxia by analysis of a mouse mutant. Proc Natl Acad Sci U S A. 2009; 106:16381–16386. [PubMed: 19805308]
24. Ma C, Schneider SN, Miller M, et al. Manganese accumulation in the mouse ear following systemic exposure. J Biochem Mol Toxicol. 2008; 22:305–310. [PubMed: 18972394]
25. Picard E, Ranchon-Cole I, Jonet L, et al. Light-induced retinal degeneration correlates with changes in iron metabolism gene expression, ferritin level, and aging. Invest Ophthalmol Vis Sci. 2011; 52:1261–1274. [PubMed: 20881284]
26. Zhang KH, Tian HY, Gao X, et al. Ferritin heavy chain-mediated iron homeostasis and subsequent increased reactive oxygen species production are essential for epithelial-mesenchymal transition. Cancer Res. 2009; 69:5340–5348. [PubMed: 19531652]
27. Ingrassia R, Lanzillotta A, Sarnico I, et al. 1B/(−)IRE DMT1 expression during brain ischemia contributes to cell death mediated by NF-κB/RelA acetylation at Lys310. PLoS One. 2012; 7:e38019. [PubMed: 22666436]
28. Tchernitchko D, Bourgeois M, Martin ME, Beaumont C. Expression of the two mRNA isoforms of the iron transporter Nramp2/DMTI in mice and function of the iron responsive element. Biochem J. 2002; 363:449–455. [PubMed: 11964145]
29. Zhang AS, Gao J, Koeberi DD, Enns CA. The role of hepatocyte hemomjuvelin in regulation of bone morphogenic protein-6 and hepcidin expression in vivo. J Biol Chem. 2010; 285:16416–16423. [PubMed: 20363739]
30. Ganz T. Systemic iron homeostasis. Physiol Rev. 2013; 93:1721–1741. [PubMed: 24137020]
31. Wang J, Pantopoulos K. Regulation of cellular iron metabolism. Biochem J. 2011; 434:365–381. [PubMed: 21348856]
32. Noetzli LJ, Carson SM, Nord AS, Coates TD, Wood JC. Longitudinal analysis of heart and liver iron in thalassemia major. Blood. 2008; 112:2973–2978. [PubMed: 18650452]
33. Delaby C, Pilard N, Puy H, Canonne-Hergaux F. Sequential regulation of ferroportin expression after erythrophagocytosis in murine macrophages: early mRNA induction by haem, followed by iron-dependent protein expression. Biochem J. 2008; 411:123–131. [PubMed: 18072938]

34. Marro S, Chiabrando D, Messana E, et al. Heme controls ferroportin1 (FPN1) transcription involving Bach1, Nrf2 and a MARE/ARE sequence motif at position -7007 of the FPN1 promoter. Haematologica. 2010; 95:1261–1268. [PubMed: 20179090]
35. Knutson MD, Vafa MR, Haile DJ, Wessling-Resnick M. Iron loading and erythrophagocytosis increase ferroportin 1 (FPN1) expression in J774 macrophages. Blood. 2003; 102:4191–4197. [PubMed: 12907459]
36. Yang F WX, Haile DJ, Piantadosi CA, Ghio AJ. Iron increases expression of iron-export protein MTP1 in lung cells. Am J Physiol Lung Cell Mol Physiol. 2002; 283:L932–939. [PubMed: 12376346]
37. Garrick MD, Dolan KG, Horbinski C, et al. DMT1: a mammalian transporter for multiple metals. Biometals. 2003; 16:41–54. [PubMed: 12572663]
38. López-Castro JD, Delgado JJ, Perez-Omil JA, et al. A new approach to the ferritin iron core growth: influence of the H/L ratio on the core shape. Dalton Trans. 2012; 41:1320–1324. [PubMed: 22134157]
39. Bomford A, Conlon-Hollingshead C, Munro HN. Adaptive responses of rat tissue isoferritins to iron administration. Changes in subunit synthesis, isoferritin abundance, and capacity for iron storage. J Biol Chem. 1981; 256:948–955. [PubMed: 7451482]
40. Ferreira C, Bucchini D, Martin ME, et al. Early embryonic lethality of H ferritin gene deletion in mice. J Biol Chem. 2000; 275:3021–3024. [PubMed: 10652280]
41. Darshan D, Vanoaica L, Richman L, Beermann F, Kühn LC. Conditional deletion of ferritin H in mice induces loss of iron storage and liver damage. Hepatology. 2009; 50:852–860. [PubMed: 19492434]
42. Sammarco MC, Ditch S, Banerjee A, Grabczyk E. Ferritin L and H subunits are differentially regulated on a post-transcriptional level. J Biol Chem. 2008; 283:4578–4587. [PubMed: 18160403]
43. White K, Munro HN. Induction of ferritin subunit synthesis by iron is regulated at both the transcriptional and translational levels. J Biol Chem. 1988; 263:8938–8942. [PubMed: 3379054]
44. Hintze KJ, Theil EC. DNA and mRNA elements with complementary responses to hemin, antioxidant inducers, and iron control ferritin-L expression. Proc Natl Acad Sci U S A. 2005; 102:15048–15052. [PubMed: 16217041]
45. Bulvik B, Grinberg L, Eliashar R, Berenshtein E, Chevion MM. Iron, ferritin and proteins of the methionine-centered redox cycle in young and old rat hearts. Mech Ageing Dev. 2009; 130:139–144. [PubMed: 18996141]
46. Ghugre NR, Enriquez CM, Gonzalez I, Nelson MD Jr. Coates TD, Wood JC. MRI detects myocardial iron in the human heart. Magn Reson Med. 2006; 56:681–686. [PubMed: 16888797]
47. Carpenter JP, He T, Kirk P, et al. On T2* magnetic resonance and cardiac iron. Circulation. 2011; 123:1519–1528. [PubMed: 21444881]
48. Kirk P, Roughton M, Porter JB, et al. Cardiac T2* magnetic resonance for prediction of cardiac complications in thalassemia major. Circulation. 2009; 120:1961–1968. [PubMed: 19801505]
49. Krijt J, Niederkofler V, Salie R, et al. Effect of phlebotomy on hepcidin expression in hemojuvelin-mutant mice. Blood Cells Mol Dis. 2007; 39:92–95. [PubMed: 17395503]
50. Latour C, Kautz L, Besson-Fournier C, et al. Testosterone perturbs systemic iron balance through activation of epidermal growth factor receptor signaling in the liver and repression of hepcidin. Hepatology. 2014; 59:683–694. [PubMed: 23907767]

- Evidence of mRNA regulation of cardiac iron transporter and storage genes in mice.
- Ferroportin mRNA increased proportionally to cardiac iron, more sharply in males than females.
- L-ferritin mRNA paralleled cardiac iron similarly in both sexes.
- H-ferritin was constitutively expressed, suggesting a natural upper limit to cardiac iron buffering.

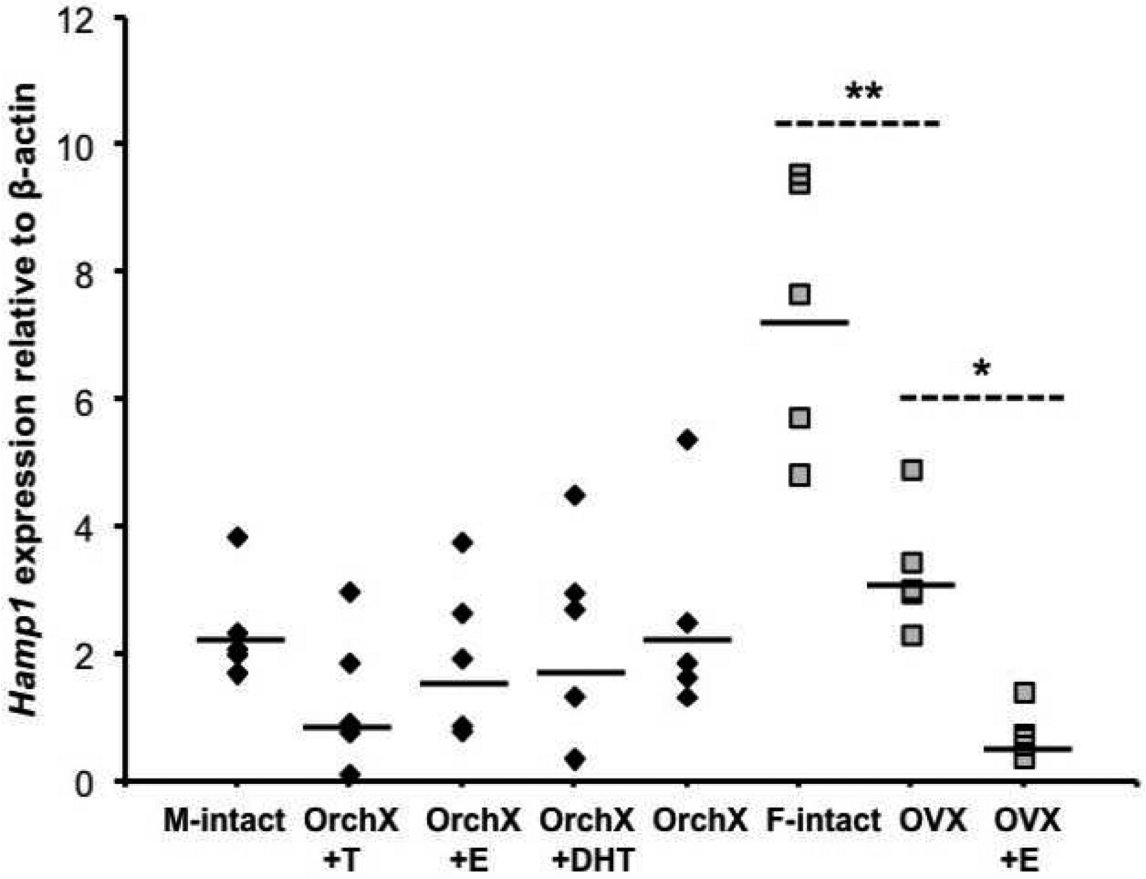

Fig 1.

Hamp1 levels in males and females. Black diamonds = males; grey squares = females. "M-intact" = gonad intact males; "F-intact" = gonad intact females. Black lines indicate geometric means. * = *Hamp1* was significantly higher in OVX versus OVX+E. ** = *Hamp1* was significantly higher in intact females versus OVX.

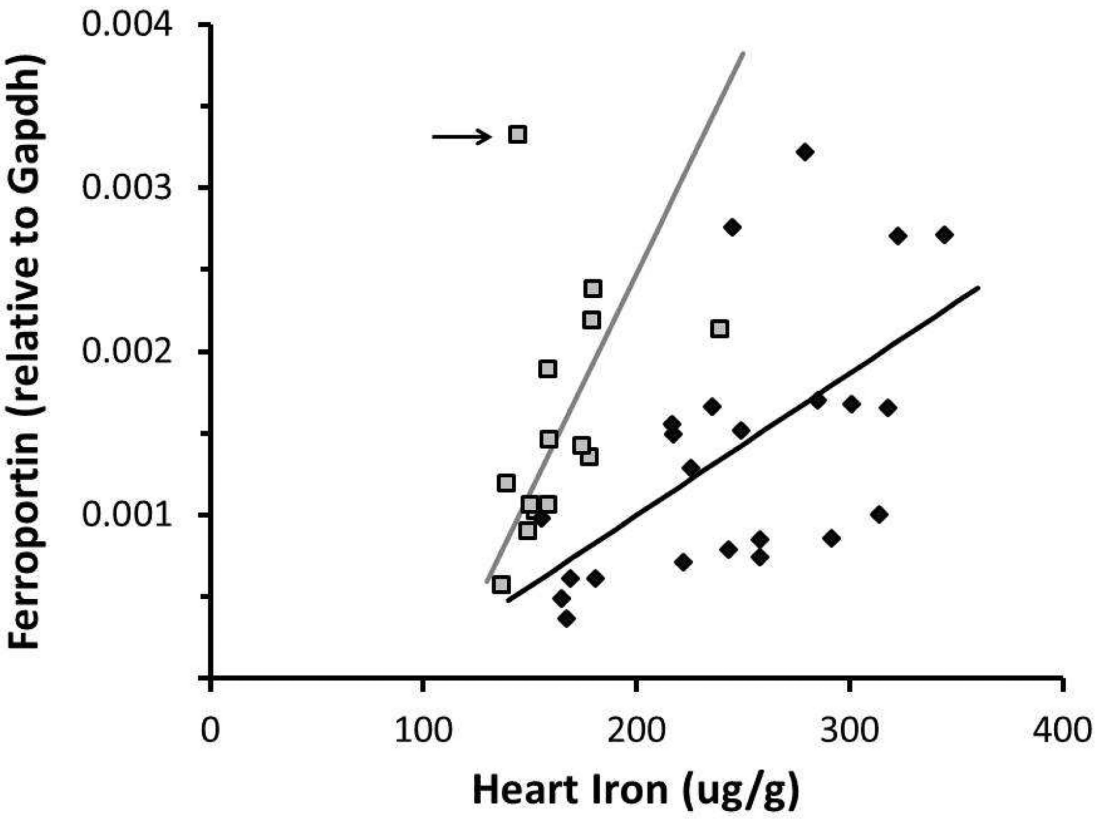

Fig 2.

Relationship between heart iron concentration and ferroportin mRNA expression in males and females. Black diamonds = males; grey squares = females. Positive correlation in males was significant (R^2=0.35, p<0.01), while the positive relationship in females did not reach significance because of one outlier (R^2=0.12, p<0.22 with outlier, R^2=0.50, p<0.01 without outlier; outlier indicated by arrow).

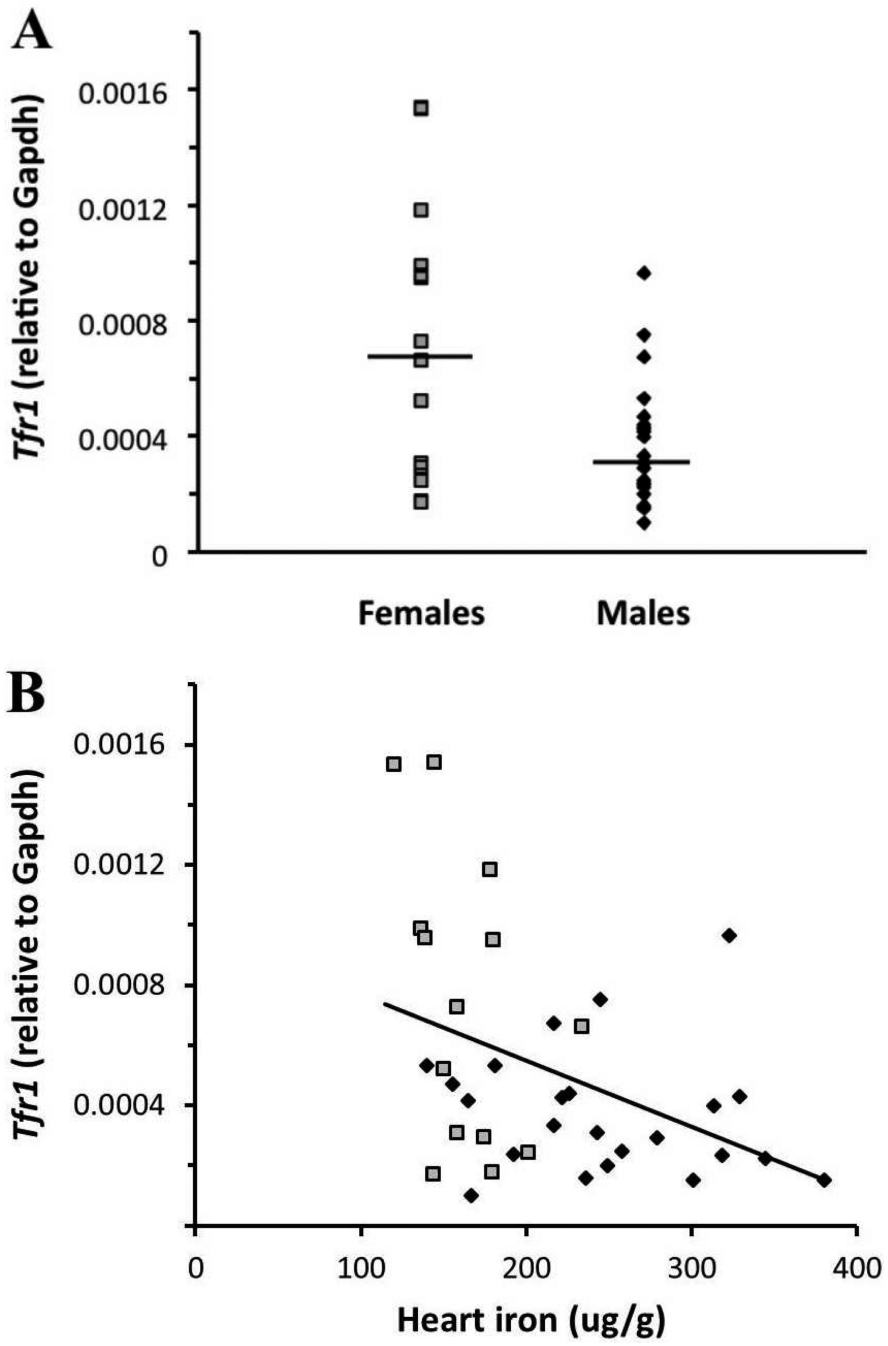

Fig 3.

Tfr1 mRNA expression and its relationship to cardiac iron concentration in males and females. Black diamonds = males; grey squares = females. (**A**) Females had significantly more *Tfr1* mRNA than males ($p<0.01$). Black lines indicate geometric means. (**B**) There was a negative correlation between *Tfr1* mRNA and heart iron concentration ($R^2=0.16$, $p<0.05$).

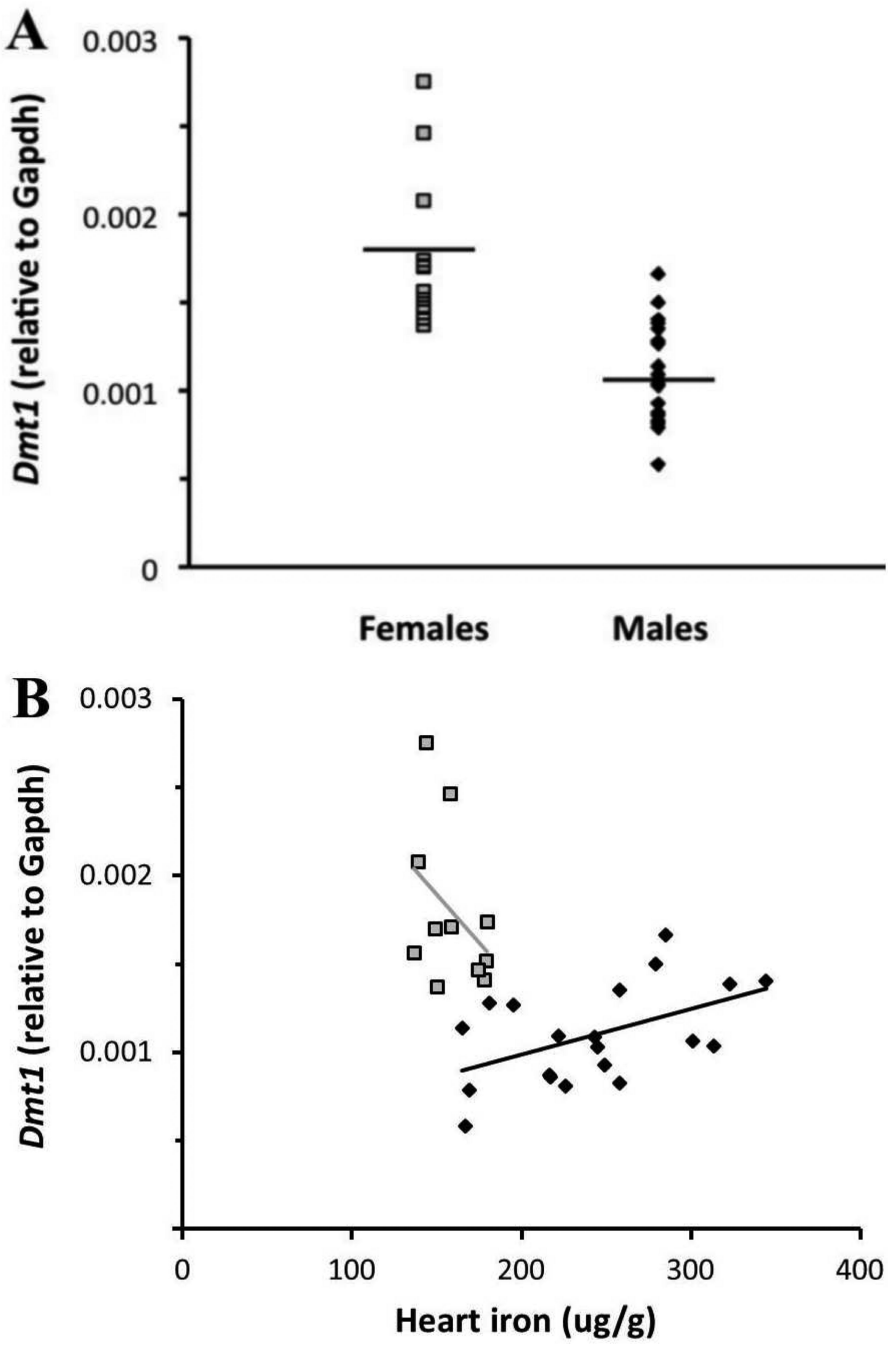

Fig 4.

Dmt1 mRNA expression and its relationship to cardiac iron concentration in males and females. Black diamonds = males; grey squares = females. (**A**) Females had significantly more *Dmt1* mRNA than males ($p<0.0001$). Black lines indicate geometric means. (**B**) Males showed a positive correlation between *Dmt1* and heart iron concentration ($R^2=0.25$, $p<0.05$).

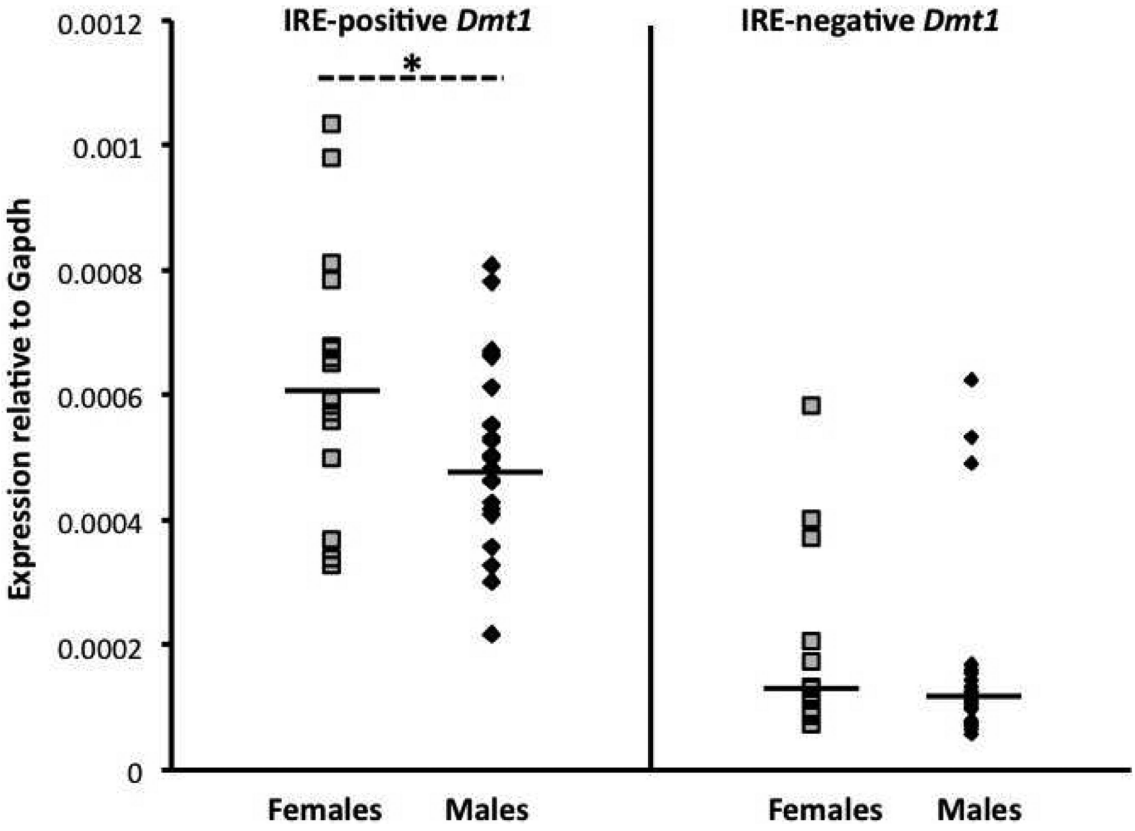

Fig 5.

mRNA expression of IRE-positive and IRE-negative *Dmt1* isoforms in male and female cardiac tissue. Black diamonds = males; grey squares = females. Black lines indicate geometric means. * = Females had significantly more IRE-positive *Dmt1* mRNA than males. Males and females had similar levels of IRE-negative *Dmt1* mRNA.

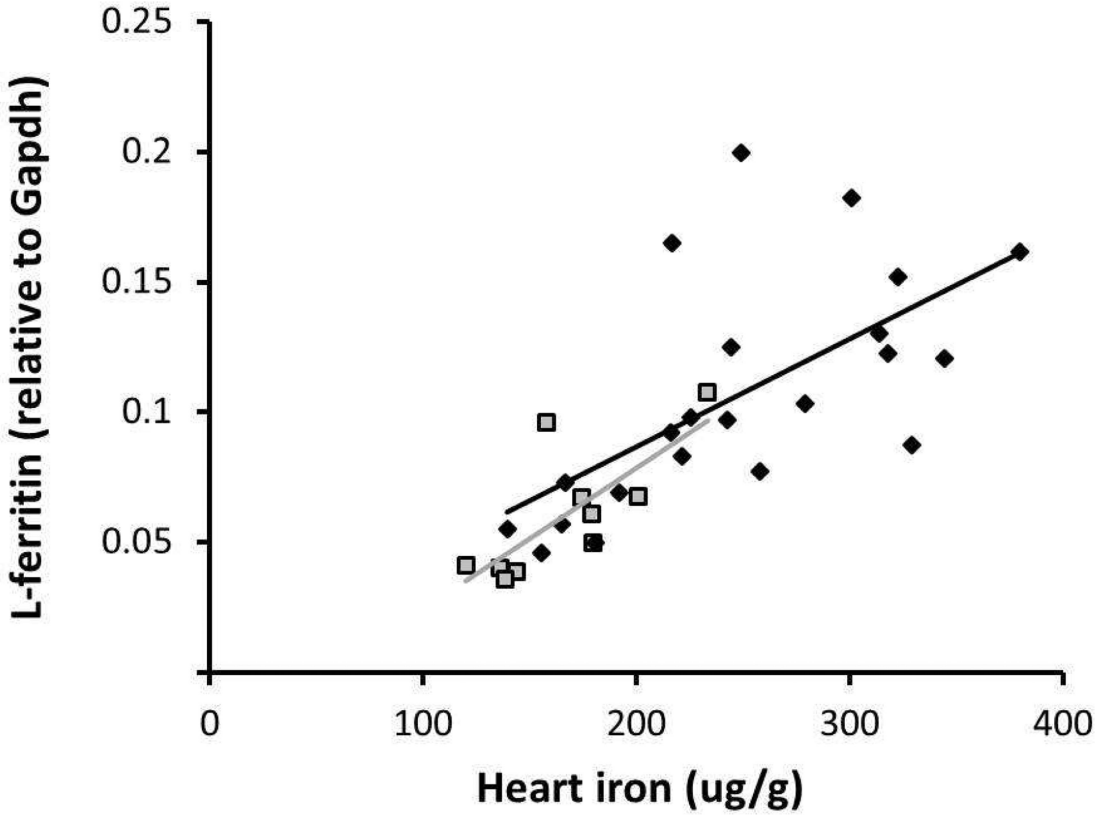

Fig 6.

L-ferritin mRNA expression and its relationship to heart iron concentration. Black diamonds = males; grey squares = females. Males and females showed very similar correlations between L-ferritin and heart iron concentration (R^2=0.41, $p<0.01$ for males and R^2=0.56, $p<0.05$ for females).

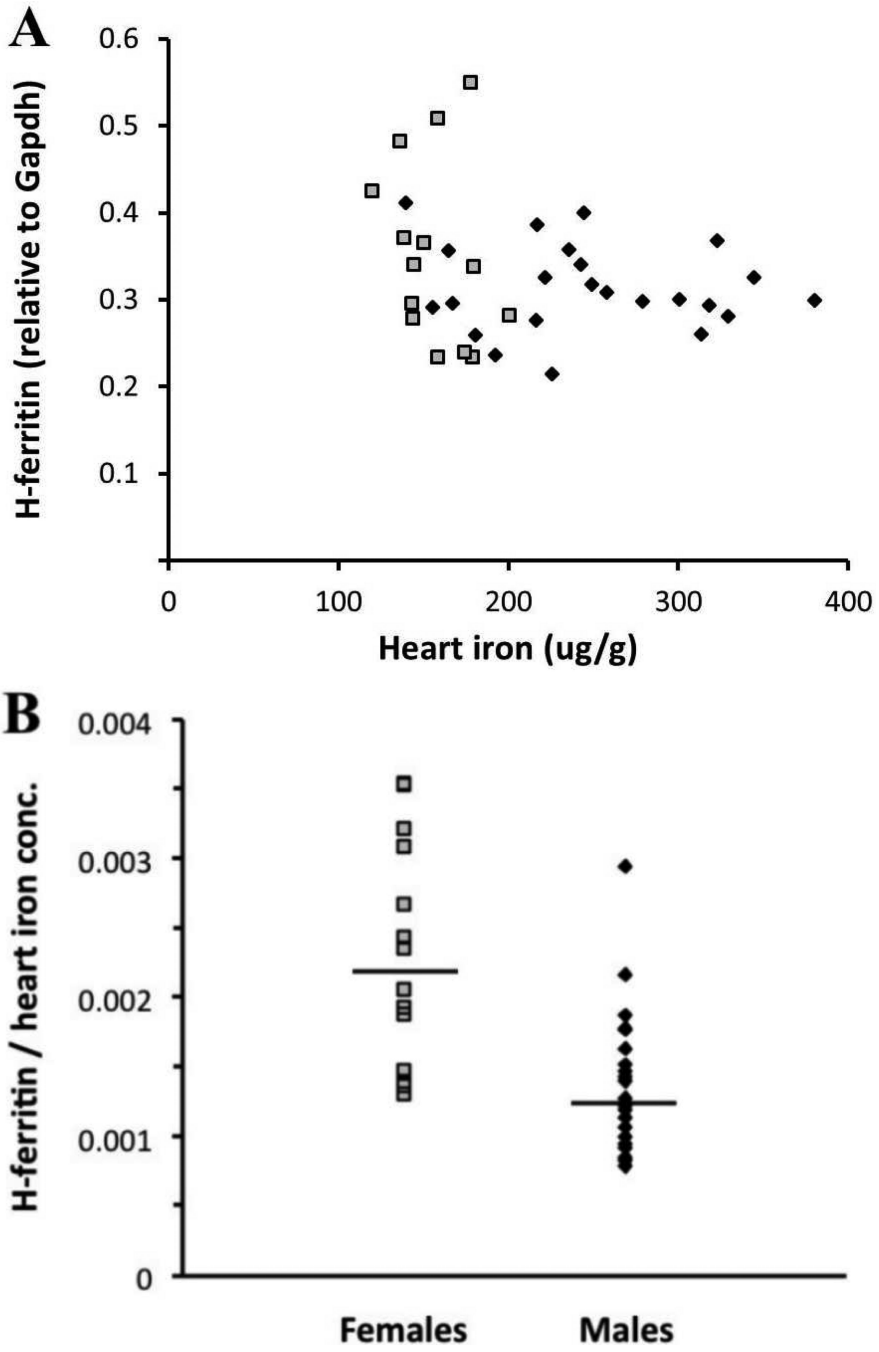

Fig 7.

H-ferritin mRNA expression and its relationship to heart iron concentration in males and females. Black diamonds = males; grey squares = females. (**A**) No correlation was found between H-ferritin and heart iron concentration in males or females. (**B**) Females had more H-ferritin mRNA when normalized to heart iron concentration ($p<0.001$). Black lines indicate geometric means.

Table 1

Iron levels, organ and body weights, and *Hamp1* expression in *Hjv*−/− and wild type mice.

Parameter	Males *Hjv*−/−	Females *Hjv*−/−	Sex Difference T-Test *Hjv*−/−	Males wild type	Females wild type	Sex Difference T-Test wild type
Heart Iron (μg/g wet weight)	238 ± 73	163 ± 29	< 0.0001	79 ± 7	82 ± 7	< 0.40
Heart Weight (g)	0.147 ± 0.026	0.131 ± 0.020	< 0.01	0.153 ± 0.012	0.128 ± 0.014	< 0.01
Liver Iron (μg/g wet weight)	2041 ± 492	1776 ± 527	< 0.05	237 ± 50	317 ± 55	< 0.05
Liver Weight (g)	1.49 ± 0.26	1.42 ± 0.29	< 0.30	1.09 ± 0.09	0.94 ± 0.15	< 0.08
Hamp1 (relative to β-actin)	1.6 ± 1.2	2.5 ± 1.3	< 0.19	26 ± 1	32 ±1	< 0.23
Body Weight (g)	26 ± 3	24 ± 2	< 0.05	28 ± 2	22 ± 1	< 0.0001

Geometric mean ± standard deviation is displayed for *Hamp1*; all other values are arithmetic mean ± standard deviation. Calculations for Hjv −/− mice include the data from all five *Hjv*−/− male groups (M-intact, OrchX+T, OrchX+E, OrchX+DHT, OrchX) and all three Hjv −/− female groups (F-intact, OVX, OVX+E).

Table 2

mRNA expression of NTBI transporters and relationship to heart iron concentration

	Expression relative to Gapdh			Hormone effect (p^*)		Correlation with heart iron concentration			
Ion channel	male	female	p^*	male	female	male		female	
						R^2	p^*	R^2	p^*
L-type	$5.1*10^3$	$5.4*10^3$	0.60	0.98	0.72	0.10	0.17	<0.01	0.84
T-type	$1.6*10^3$	$1.7*10^3$	0.75	0.56	0.42	<0.01	0.75	<0.01	0.98
Zip 14	$4.0*10^3$	$3.7*10^3$	0.20	0.18	0.93	<0.01	0.69	0.17	0.21

In the “hormone effect” column, p-values were calculated via ANOVA of all male groups (OrchX, OrchX+T, OrchX+E, OrchX+E, intact) or all female groups (OVX, OVX+E, intact) for a given ion channel's mRNA expression.

* p-value.